Published in final edited form as:
Biomaterials. 2009 December ; 30(36): 6996–7004. doi:10.1016/j.biomaterials.2009.09.001.

Gene Delivery via DNA Incorporation Within a Biomimetic Apatite Coating

L. N. Luong[1], **K. M. McFalls**[1], and **D. H. Kohn**[1,2,*]

[1] Biomedical Engineering, University of Michigan, Ann Arbor, MI 48109, USA

[2] Biologic & Materials Sciences, University of Michigan, Ann Arbor, MI 48109, USA

Abstract

Integrating inductivity with conductivity in a material may advance tissue engineering. An organic/inorganic hybrid was developed by incorporating plasmid DNA encoding for the β-gal gene complexed with Lipofectamine 2000® (DNA-Lipoplex) within apatite via coprecipitation. It is hypothesized that this system will result in enhanced transfection efficiency compared to DNA-Lipoplexes adsorbed to the mineral surface and DNA coprecipitated without Lipofectamine 2000®. PLGA films were cast onto glass slips and apatite and DNA were coprecipitated in modified simulated body fluid (mSBF). DNA-Lipoplex presence in mineral, DNA-Lipoplex stability (vs. coprecipitation time), and transfection efficiency (determined with C3H10T1/2 cells) as a function of coprecipitation time, DNA-Lipoplex concentration, and DNA incorporation method were studied. DNA-Lipoplex presence and spatial distribution on apatite were confirmed through fluorescence. Transfection efficiency was highest for 6 h of DNA- Lipoplex coprecipitation. Differences in transfection efficiency were found between the DNA concentrations, with the highest efficiency for coprecipitation being 40 μg/ml ($p \leq 0.009$ relative to other coprecipitation concentrations). Significant differences in transfection efficiency existed between incorporation methods ($p < 0.05$) with the highest efficiency for DNA-Lipoplex coprecipitation. This hybrid material system not only integrates inductivity provided by the DNA and conductivity provided by the apatite, but it also has significant implications in non-viral gene delivery due to its ability to increase transfection efficiency.

Keywords

coprecipitation; biomineralization; biomimetic material; DNA; lipid; SBF (simulated body fluids)

1. Introduction

The clinical basis for developing strategies to regenerate bone is the healing of bone defects caused from trauma, congenital malformations, and progressively deforming skeletal disorders. Bone tissue engineering provides an alternative to bone grafting and direct usage of growth factors to regenerate bone. An ideal bone tissue engineering approach would incorporate osteoconductivity and osteoinductivity potential into the design of the supporting biomaterial, as well as biocompatibility, degradability, mechanical integrity, and the ability to support cell transplantation.

*Corresponding author: Tel.: +1-734-764-2206; fax: +1-734-647-2110. dhkohn@umich.edu (D. H. Kohn).

Direct bonding between implants and bone, the ultimate goal of osteoconductivity, can occur if a layer of bone-like mineral forms on the surface of the implant [1]. It has therefore been hypothesized that formation of a bone-like mineral layer within the pores of a tissue engineering scaffold may enhance the conduction of host cells into scaffolds [2], and also enhance osteogenic differentiation of cells transplanted on scaffolds [3]. The bone-like mineral enhances the osteoconductivity and mechanical properties of the scaffold and can serve as a cell transplantation vehicle [2]. Bone-like mineral coatings can also serve as carriers for inductive agents [2,4], providing a platform for the three tissue engineering approaches of conduction, induction, and cell transplantation.

The coprecipitation of biological factors and bone-like mineral has been used to incorporate growth factors on metal substrates, such as titanium alloy implants [5–7]. An important advantage to coprecipitation is the ability to form calcium phosphate coatings at a physiological temperature, minimizing conditions that would degrade the biological activity of the factors [8–11]. For example, the biological activity of bovine serum albumin, tobramycin, and recombinant human bone morphogenetic protein 2 (BMP-2) is retained when each of these biomolecules is coprecipitated with calcium phosphate onto titanium [6,7,12]. More specifically, BMP-2 coprecipitated into biomimetic apatite coatings can induce ectopic bone formation *in vivo* [13]. The ability to increase the loading efficiency and to control the spatial localization of proteins within bone-like mineral coatings has also been demonstrated utilizing coprecipitation [14].

Gene therapy is one approach to achieve the design objective of integrating inductivity into a material. Gene delivery provides an alternative to utilizing proteins, and has advantages over protein delivery, including a longer half-life, and lower expense [15]. The incorporation of genes into cells can be achieved virally and non-virally [16–19]. However, viral approaches present disadvantages, including the risk of mutations, insert size limitations, and viral-induced immune responses [15]. An alternative is the use of non-viral methods, such as naked DNA, cationic polymers, and cationic lipids [16,20,21]. While non-viral methods are less efficient than viral techniques, they are more promising in terms of accommodating larger genes of interest, lower immunogenicity, and the potential for tissue targeting [15,22]. An optimal non-viral gene delivery system will fulfill the following design objectives: 1) the carrier should avoid aggregation or negative interactions with the extracellular matrix, 2) the carrier should condense the DNA to facilitate cellular internalization, and 3) cellular processes to transcribe and translate the gene of interest should not be inhibited [15].

Non-viral gene delivery has been achieved by complexing DNA with cationic lipids [17], as well as precipitating DNA with calcium phosphate [23,24]. However, the two approaches of cationic lipids and calcium phosphate precipitation have not been combined. Cationic lipids are typically composed of a positively charged head group, a hydrophobic chain, and a linker group [25]. The positively charged lipids interact with the negatively charged DNA chains, resulting in complexes. The cellular uptake of these complexes depends on their stability and size [25]. For example, Lipofectamine 2000®, which is a lipid based transfection agent for eukaryotic cells, protects the DNA from enzymatic digestion from DNase treatment [26], whereas plasmid DNA alone is prone to degradation by nucleases [15]. DNA-Lipoplexes are therefore successful in cellular transfection, both *in vitro* and *in vivo* [27,28].

The precipitation of DNA/calcium phosphate nanocomposites has also been successful in inducing transfection of cell lines, due to the concentrated quantity of DNA localized in the immediate cellular environment [20,24]. The precipitation of a calcium phosphate coating onto a polymer scaffold increases the stiffness of the scaffold [2] and increased substrate stiffness increases cellular uptake of DNA condensates [29]. These advantages of calcium phosphates

can be combined with the advantages of cationic lipids by coprecipitating coatings of calcium phosphate and DNA-Lipoplexes onto a biomaterial substrate.

In this study, we developed an organic/inorganic hybrid by coprecipitating plasmid DNA encoding for the β-galactosidase gene complexed with a cationic lipid (Lipofectamine 2000®) and biomimetic apatite onto a polymer substrate. The lipid condenses the DNA, better enabling cellular uptake, while the coprecipitation of DNA-Lipoplexes with mineral localizes high, homogeneously dispersed concentrations of DNA in the immediate cellular environment. We hypothesized that this combinatorial inductive/conductive system would result in enhanced transfection efficiency compared to DNA-Lipoplexes adsorbed to the mineral surface and DNA coprecipitated without Lipofectamine 2000®. To test this hypothesis, experiments were conducted to address: 1) DNA-Lipoplex presence in mineral, 2) DNA-Lipoplex stability (vs. coprecipitation time), and 3) transfection efficiency (determined with C3H10T1/2 cells) as a function of coprecipitation time, DNA-Lipoplex concentration, and DNA incorporation method.

2. Materials and Methods

2.1 PLGA film preparation

The films were prepared using 5 wt. % PLGA, 85:15 PLA:PGA ratio (Alkermes), in chloroform solution. The films (approximately 200–300 μm thick) were cast onto 15 mm round glass coverslips, covered with aluminum foil and air dried for at least 24 hours under a fume hood. Prior to mineralization, the films were etched in 0.5 M NaOH for seven minutes. They were rinsed thoroughly with Millipore water before use.

2.2 Modified simulated body fluid

A modified simulated body fluid (mSBF, which contains 2X the concentration of Ca^{2+} and HPO_4^{2-} as standard SBF) was used to mineralize the films [14]. mSBF consists of the following reagents dissolved in Millipore water: 141 mM NaCl, 4.0 mM KCl, 0.5 mM $MgSO_4$, 1.0 mM $MgCl_2$, 4.2 mM $NaHCO_3$, 5.0 mM $CaCl_2{\cdot}2H_2O$, and 2.0 mM KH_2PO_4. mSBF was prepared at 25°C and titrated to pH 6.8 using NaOH to avoid homogeneous precipitation of calcium phosphate.

2.3 Plasmid DNA preparation and purification

Plasmid DNA encoding for β-galactosidase (β-gal) was produced via the transformation of E. Coli competent cells (Promega #L2001). Plasmid DNA purification was completed using the protocol provided by Qiagen. Cells were harvested from 500 ml of LB broth. Following centrifugation and cell lysis, the purified DNA was precipitated by isopropanol. DNA pellets were washed with ethanol, dried, resuspended in TE buffer at pH 8.0, and stored at −20°C.

2.4 Complexing plasmid DNA to Lipofectamine 2000®

DNA-Lipofectamine 2000® complexes (DNA-Lipoplex) were prepared in polypropylene centrifuge tubes according to the protocol provided by the manufacturer (Molecular Probes, Invitrogen). The ratio of complexation was 3 μl of Lipofectamine 2000® per μg of plasmid DNA. Briefly, the DNA and the Lipofectamine 2000® were individually diluted in Opti-MEM Reduced Serum Medium and gently mixed. The samples were then incubated for 5 minutes at room temperature, after which they were combined together. The DNA-Lipofectamine 2000® mixture was then incubated for 20 minutes at room temperature.

2.5 Mineralization and DNA incorporation methods

Four types of samples were prepared: PLGA coated with mineral, PLGA with DNA incorporated, PLGA coated with mineral and coprecipitated DNA-Lipoplexes, and PLGA coated with mineral and DNA-Lipoplexes adsorbed to the mineral surface. PLGA covered glass slips were submerged into each Petri dish containing 50 ml of mSBF. Mineralization was carried out for 3 to 4 days at 37°C and the solutions were exchanged daily in order to replenish the ion concentration to supersaturated levels. For coprecipitation of mineral-DNA and mineral-DNA- Lipoplexes, the mineralization scheme to deposit the precursor mineral layer was the same (i.e. the starting point for coprecipitation was similar). Samples were removed from the Petri dishes after mineralization and placed into 24 well plates. An mSBF solution containing DNA-Lipoplexes or DNA alone was then added to the samples (1 ml per sample). Concentration and coprecipitation time were dependent on the experiment performed as detailed in Sections 2.6 to 2.10. Coprecipitation was carried out at 37°C; the samples were placed on a rotational shaker to evenly distribute the complexes (approximately 50 rpm). For the DNA incorporated into PLGA, the DNA was added to the 5 wt. % PLGA, 85:15 PLA:PGA ratio (Alkermes), in chloroform solution. The films were cast onto 15 mm round glass coverslips (250 μl), covered with aluminum foil and air dried for at least 24 hours under a fume hood. DNA-Lipoplexes incorporated into PLGA was not included due to the inability to achieve the required composition of DNA-Lipoplexes in PLGA/chloroform solution. For DNA-Lipoplex adsorption to mineral, the complexes were prepared in the Opti-MEM media and pipetted onto the surface of the mineralized substrate.

2.6 Plasmid DNA incorporation and effects on mineral morphology

Effects of DNA incorporation on mineralization were examined using scanning electron microscopy (Philips XL30 FEG Scanning Electron Microscope). The following groups were examined: 1) Mineralized controls, 2) Plasmid DNA coprecipitated with mineral onto films, 3) Plasmid DNA-Lipoplex adsorbed to mineralized films, and 4) Plasmid DNA-Lipoplex coprecipitated with mineral onto films. Films were coated with a thin layer of gold and examined at 3 kV.

2.7 Verification of Plasmid DNA presence and spatial distribution

The spatial distribution of the DNA was determined using a fluorescence microscope (Nikon TE 3000 Inverted Microscope). The following groups were examined: 1) Mineralized controls, 2) Plasmid DNA incorporated into PLGA, 3) Plasmid DNA coprecipitated with mineral, 4) Plasmid DNA-Lipoplex adsorbed to mineralized films, and 5) Plasmid DNA-Lipoplex coprecipitated with mineral. For this qualitative assessment, ten μg of plasmid DNA was used per sample. For the coprecipitation groups, 10 μg was the DNA concentration in solution and the samples were incubated at 37°C for 24 h. Samples were then removed and dried in the chemical fume hood. Bisbenzimide Hoescht (Sigma-Aldrich) was used to determine the spatial distribution of the plasmid DNA, while DiO Cell Labeling Solution (MicroProbes, Invitrogen) was used to determine the presence of the Lipofectamine 2000®. Briefly, a 1:500 dilution of Hoescht and a 1:200 dilution of DiO solution were made using 1X PBS. Samples were placed into 24 well plates, and rewet with ddH_2O, which was then removed. Staining solution was placed over the samples; the plate was covered with aluminum foil and incubated for 30 minutes at 37°C. Solution was then removed and the samples were rinsed 4 to 5 times with ddH_2O. Samples were placed on glass microscope slides with GelMount (Biomedia) as a mounting medium. Samples were imaged on the same day on a fluorescence microscope with emission wavelengths of 420 and 510–560 nm for DNA and Lipofectamine 2000®, respectively.

2.8 Plasmid DNA stability and Plasmid DNA- Lipofectamine 2000® complex stability

To determine the stability of the complexes formed, gel electrophoresis (based on size) and transfection efficiency at varying timepoints (6, 12, 24 and 48 h) were examined. All samples were prepared in polypropylene tubes. At first, the stability of the plasmid DNA in water was examined to determine its intrinsic stability. The protocol was then repeated to examine DNA – Lipofectamine 2000® complexation in Opti-Mem. The tubes were placed in an incubator at 37°C. Samples were then removed at each timepoint and frozen (DNA in water) or stored at 4°C (DNA-Lipoplex in Opti-Mem). Samples were placed in wells in a 0.6% agarose gel containing ethidium bromide. Freshly thawed (no previous incubation) plasmid DNA and plasmid DNA conjugated to Lipofectamine 2000® were prepared as controls. Samples were loaded and run for 75 minutes at 80V, and images were obtained and analyzed using a Fluor S MultiImager (Bio-Rad, CA).

To determine plasmid DNA-Lipoplex stability in the mSBF during and after the precipitation of the apatite and complexes with respect to time of coprecipitation, a second set of experiments was performed using the mouse embryonic fibroblast cell line C3H10T1/2 (provided by Dr. Franceschi, University of Michigan). The C3H10T1/2 cell line was chosen due to its capability of differentiating along the osteogenic lineage with either exogenous protein or via gene transfection [30,31]. Samples (n=4) were prepared as stated in Section 2.5 using coprecipitation times of (6, 12, 24, and 48 h). The baseline concentration for the samples was 10 μg in 1 ml of mSBF per sample. At each incubation timepoint, the samples were removed and rinsed with HBSS (Hanks buffered saline solution).

MEMα medium (Invitrogen) containing 10% fetal bovine serum (FBS) without antibiotics was prepared, and one day before transfection, the cells were replated at a density of 50,000 in 1 ml of media. The plates were gently rocked to evenly distribute the cells on the surface of the films and placed in the incubator at 37°C. The media was exchanged after 24 hours. The total time allowed for transfection was 48 hours. Media was aspirated and the cells were washed with PBS.

Cells were fixed for 15 min with a 0.25% v/v glutaraldehyde solution and then rinsed gently 3 times with PBS. X-gal staining solution containing N,N-DMF, $MgCl_2$, $K_4Fe(CN)_6$ $3H_2O$, and $K_3Fe(CN)_6$ was added to each well containing cells and incubated at 37° C between 14–16 hours. The X-gal solution was then removed and the samples were rinsed 2–3 times with PBS. Samples were removed and placed onto microscope slides and mounted using GelMount. Samples were then observed under the light microscope. Fifteen random locations per sample were imaged, and then positively stained cells were counted. The average number of stained cells per location was then applied to the entire area of the well resulting in the total number of cells that were stained. The cellular transfection efficiency is based on the total number of stained cells in the well divided by the initial seeding density of 50,000 cells.

2.9 Effect of plasmid DNA concentration on transfection efficiency

To determine the plasmid DNA-Lipoplex concentration needed to obtain the highest transfection efficiency, coprecipitation and adsorption were examined. For coprecipitation, the concentration was varied (0, 10, 20, or 40 μg) in 1 ml of 1X mSBF. For adsorption, the adsorption solution contained 0, 10, 20, or 40 μg of DNA-Lipoplexes. Samples (n=4) were prepared as stated in Section 2.5. Coprecipitated and mineralized control samples were incubated at 37 °C. The DNA-Lipoplexes were adsorbed onto mineralized films during the corresponding coprecipitation time period. After 6 h, the samples were removed and rinsed with HBSS. The C3H10T1/2 cell seeding density was 50,000 per sample with 1 ml of media. Fixing, staining, and analysis were the same as stated in Section 2.8.

2.10 Effect of plasmid DNA incorporation technique on transfection efficiency

The transfection efficiencies of the following methods of DNA incorporation were examined: 1) PLGA only, 2) Plasmid DNA incorporated into PLGA, 3) Mineralized controls, 4) Plasmid DNA coprecipitated with mineral, 5) Plasmid DNA-Lipoplex adsorbed to mineral, and 6) Plasmid DNA-Lipoplex coprecipitated with mineral. The DNA or DNA-Lipoplex concentration was 40 μg (in 1X mSBF, adsorption solution, or in PLGA). Samples (n=4) were prepared as stated in Section 2.5. All of the samples containing mineral and controls (except adsorption) were incubated at 37 °C. The DNA-Lipoplexes were adsorbed during the corresponding coprecipitation time period. After 6 h, the samples were removed and rinsed with HBSS. The cell seeding density was 50,000 per sample with 1 ml of media. Fixing, staining, and analysis were the same as stated in Section 2.8.

2.11 Statistical analysis

The Kruskal-Wallis One Way ANOVA on Ranks and/or ANOVA were used to analyze the differences in transfection efficiency of the C3H10T1/2 cells with variations in coprecipitation time, DNA-Lipoplex concentration, and incorporation method. The Student Newman Keuls post hoc comparison test was used for pair-wise comparisons.

3. Results

3.1 Presence and localization of DNA and DNA-Lipoplexes in biomimetic apatite

At low magnification, the macroscopic mineral morphology was similar for all sample groups. The nucleation sites were approximately 10–15 μm in diameter (Figure 1). However, at higher magnification, morphological differences were more apparent. Mineralization resulted in the deposition of plate-like structures (Figure 2a). The coprecipitation of DNA and adsorption of DNA-Lipoplexes did not change the morphology of the plates (Figure 2b,c) from that of the mineralized controls. Incorporation of DNA-Lipoplexes via coprecipitation (Figure 2d) resulted in plate-like crystals that were covered by a “fibrous” coating (black arrows in inset), thickening the plate-like structures (white arrows), compared to samples in which only DNA was coprecipitated or the mineralized controls.

The presence of both the plasmid DNA and the lipid transfection agent within the mineralized substrate was verified (Figure 3). The mineralized controls that did not contain DNA or cationic lipid, did not exhibit fluorescence (Figure 3, a–b). Incorporating DNA into PLGA resulted in the detection of bubbles from DNA staining, but no staining for the lipid transfection agent was detected (Fig 3, c–d). Plasmid DNA incorporation via coprecipitation resulted in an even distribution of DNA fluorescence over the entire substrate, and also demonstrated an absence of the lipid transfection agent (no red fluorescence) (Figure 3, e–f). The superficial adsorption of the DNA-Lipoplexes onto the surface of the mineralized films resulted in fluorescence for both DNA and lipid, however the areas of fluorescence are localized and limited (Figure 3, g–h). Only for the DNA-Lipoplex coprecipitation samples was an even distribution of fluorescence demonstrated for both DNA and lipid (Figure 3, i–j). The surface adsorption and coprecipitation of DNA-Lipoplexes demonstrated the colocalization of the DNA and the lipid as actual complexes in addition to free plasmid DNA that was not bound to complexes.

3.2 Plasmid DNA stability in water and DNA-Lipoplex complexation in medium

The plasmid DNA encoding for the β-galactosidase gene has a base-pair length of 7504 bp. As incubation time in water increased, the stability of the plasmid DNA decreased (Figure 4, a–b). As the band (ca. 6557), which is representative of the supercoiled form of the plasmid DNA, decreased in intensity with increasing incubation time, another secondary band (between 9416 and 23130 bp, representing nicked circular form of DNA) formed and increased in

intensity with increasing incubation time (Figure 4, a–b). DNA stability is demonstrated by these changes in supercoiled and nicked circular DNA, where the supercoiled form is preferred for gene transfection.

The formation of the DNA-Lipoplexes in Opti-Mem was visually confirmed via gel electrophoresis (Figure 4c). The complexation of the plasmid DNA to the transfection agent was almost complete, due to the absence of bands in all lanes containing the DNA-Lipoplexes. Due to size-exclusion effects, the complexes remained in the wells. The bright outlines surrounding the wells containing the DNA-Lipoplexes compared to the lane containing only DNA (outline is not present) are also represented by the intensity profiles of 2 lanes: DNA 0 h and DNA-Lipo 48 h (Figure 4d). The two peaks denote the top and bottom edges of the wells, and the intensities were higher for the DNA-Lipoplex lane compared to the DNA only lane (highest peak representing the DNA is shown in the inset image), which suggests the size exclusion effect.

3.3 Effects of coprecipitation time on DNA-Lipoplex stability

The ability of these complexes to be uptaken by the cells and then translated was not affected by the coprecipitation time (Figure 5). There were no significant differences among the four coprecipitation time periods ($p=0.084$). Based on the results from DNA stability (Figure 4) the time of coprecipitation was limited to 6 hours for the remaining experiments.

3.4 Effects of adsorption/coprecipitation concentration on DNA-Lipoplex transfection

Varying the concentrations of the DNA-Lipoplexes during adsorption and coprecipitation resulted in significantly different transfection efficiencies, $p=0.004$ and $p<0.001$ respectively (Figure 6). Significantly different transfection efficiencies ($p<0.05$) existed between adsorption concentrations, except between 20 μg and 40 μg, with the highest transfection efficiency corresponding to a concentration of 10 μg. Significantly different transfection efficiencies ($p\leq0.009$) existed between coprecipitation concentrations, except between 10 μg/ml and 20 μg/ml, with the highest transfection efficiency corresponding to a DNA-Lipoplex concentration of 40 μg/ml. Coprecipitation resulted in significantly higher transfection efficiencies than adsorption for 20 μg/ml and 40 μg/ml ($p<0.05$).

3.5 Effects of incorporation method on DNA-Lipoplex transfection

Varying the incorporation method for the DNA resulted in significantly different transfection efficiencies, $p<0.001$ (Figure 7). The coprecipitation of DNA-Lipoplexes resulted in the highest transfection efficiency compared with all groups ($p<0.05$). The transfection efficiency of the DNA-Lipoplex adsorption group was significantly increased when compared with all groups ($p<0.05$), except the DNA-Lipoplex coprecipitation group. The higher transfection efficiency of the DNA-Lipoplex adsorption group compared to the DNA only coprecipitation group suggests that the addition of the cationic lipid enhances transfection. Higher transfection efficiency for coprecipitation compared to adsorption suggests higher availability of the complexes on the surface of the apatite.

4. Discussion

The focus of this study has been on the development of an organic/inorganic hybrid that incorporates plasmid DNA complexed with a cationic lipid into biomimetic apatite via coprecipitation. This hybrid can be formed at physiological pH, temperature, and pressure. The advantages of combining the methods of calcium phosphate based transfection and cationic lipid assisted transfection are many fold: the biomimetic mineral increases substrate stiffness and osteoconductivity in addition to serving as a carrier for the DNA which increases osteoinductivity. The presence of the lipid condenses the DNA, making cellular internalization

easier (Figure 7), while the deposition of apatite with the DNA-complexes provides for higher, homogeneously distributed concentrations of DNA available for cellular uptake (Figure 3).

Coprecipitation of the DNA-Lipoplexes displayed the highest transfection efficiency compared to all other incorporation techniques, including coprecipitation of the plasmid alone (Figure 7). The transfection efficiency of the adsorbed DNA-Lipoplexes was higher than that of coprecipitated DNA (Figure 7), which is suggestive of the enhancement in transfection that the cationic lipid complexation provides. This increase in transfection efficiency with cationic lipid is possibly caused by the change in charge and size of the DNA [32,33]. A cationic lipid agent can promote the condensation of DNA particles, protect the DNA from degradation, and enhance cellular uptake [22,34]. Transport across the nucleus is limited to particle diameters less than 26 nm [35]. After condensation using cationic lipids, diameters of approximately 23 nm have resulted [32], thus enhancing cellular internalization. For example, polyethyleneimine (PEI), a cationic polymer, enables DNA encoding for bone morphogenetic protein 4 to condense, which significantly increases the mineral density of regenerated bone compared to uncondensed DNA [16].

Transfection efficiency is also DNA-Lipoplex concentration dependent. For coprecipitation, higher concentrations of DNA-Lipoplexes tended towards higher transfection efficiencies (Figure 6). However for adsorption, the reverse was true. The different trends in transfection efficiency may be due to the ability of coprecipitation to better retain the complexes on the mineral compared to adsorption [14], suggesting the presence of a stronger interaction between the complexes and apatite during coprecipitation. This enhanced retention of DNA-Lipoplexes at the apatite surface with coprecipitation leads to a higher surface density, which enhances transfection efficiency [20,34,36]. With adsorption, the lower transfection efficiencies may be the result of DNA-Lipoplexes aggregating at higher concentrations without the opportunity for the complexes to be evenly dispersed (Figure 3). Alternatively, there may be a lower affinity between the complexes and the apatite surface during adsorption compared to coprecipitation, therefore less complexes adsorb.

DNA stability is essential for the retention of biological activity and DNA topology may serve an important role in transfection ability. Plasmid DNA can be found in different forms, the most common of which are supercoiled, nicked circular, and linearized [37]. The supercoiled form is the most condensed conformation; nicked circular results in the loss of the supercoiling capability; and linearized DNA forms when the strands are cleaved. Over the time of incubation in water, DNA stability decreased, resulting in less of the supercoiled form of DNA and more of the nicked circular form (Figure 4). Supercoiled DNA, when complexed to a cationic polymer exhibits higher transfection efficiencies compared to nicked circular or linearized DNA forms [38]. Therefore, longer coprecipitation times could lead to lower transfection efficiencies due to the change in DNA conformation. Complexation in medium was demonstrated to be complete by the absence of bands since free DNA that did not complex would be visible as a band [26]. Incubation in medium over time did not result in the dissociation between the DNA and the cationic lipid. Stability of the DNA-Lipoplexes was also tested by assessing the transfection efficiency using C3H10T1/2 cells at four coprecipitation times. There was no significant difference in transfection efficiency with increasing time of incubation (Figure 5). To minimize the possibility of DNA instability (Figure 4a), the coprecipitation time for future experiments was limited to 6 hours. Additionally, a precursor layer of mineral was applied before initiating the coprecipitation process since longer periods of incubation of the DNA-Lipoplexes in mSBF may cause DNA instability, and therefore decrease the transfection efficiency. In general, the supercoiled form of DNA is preferred for gene transfections; however, the presence of nicked circular DNA may not always decrease transfection efficiency in specific cases [39].

By coprecipitating the DNA-Lipoplexes into the mineral, the morphology of the mineral changed, while adsorption of DNA-Lipoplexes or coprecipitation of just DNA did not change the plate-like mineral (Figure 2). The distinctive morphological features resulting from the coprecipitation of the DNA-Lipoplexes with apatite demonstrate the interactions that occur between the complexes and the mineral plates. The presence of a “fibrous” coating (Figure 2d) is most likely due to the presence of the cationic lipid, because the coprecipitation of DNA alone resulted in minimal differences in apatite morphology compared to the mineralized controls. Condensation via cationic particles can result in the formation of toroids or rods [40,41], which is a possible cause for the “fibrous” coating displayed on the plate-like mineral. Even after thorough rinsing, the DNA-Lipoplexes were still retained on the apatite especially for the coprecipitation groups (Figure 3). Coprecipitation may therefore lead to DNA-Lipoplex incorporation into the three dimensional crystal latticework resulting in the morphological changes observed. It is probable that the interaction is between the positively charged Ca ions within the apatite and the negatively charged backbone of the DNA [42]. It has also been hypothesized that affinity binding can occur between DNA and hydroxyapatite crystals [42]. The interaction between the DNA-Lipoplexes and the mineral via coprecipitation may enhance the availability of these complexes for cellular uptake. In addition to better retention, coprecipitation also distributes protein through the thickness of the apatite compared to just placing it at the apatite surface as is the case with adsorption [14]. Therefore, coprecipitation offers an added advantage of prolonging delivery.

Transfection efficiencies are low (~5–12%), which is typical of a non-viral gene delivery method when compared to viral delivery methods. However, utilizing non-viral gene delivery is advantageous in regards to ease of reproduction without the risk of mutation [22]. Different methods of cationic carrier based gene delivery (lipid, gelatin, and PEI) have transfection efficiencies ranging from ca. 3% to 18%, which are dependent on both the method of delivery and the cell type utilized [43]. Generally, the transfection efficiencies that are typical of all non-viral methods are not high enough for *in vivo* gene therapy. However, lipid based gene transfection has induced new bone tissue *in vivo* with and without cell transplantation [17,28, 44]. Therefore, DNA-Lipoplex coprecipitation has the potential to become a viable method for gene therapy.

Transfection efficiency is controlled by a combination of factors, including cell type, DNA topology, mechanism of cellular internalization, and cytoplasmic barriers including degradation via nucleases [20,36,45,46]. More established cell lines are easier to transfect compared to primary cells [43]. Cells in the mitotic phase exhibit decreased uptake of DNA complexed to cationic lipids in comparison to cells in the interphase [45]. Cell cycle varies between cell types, therefore the use of a different cell line may lead to higher transfection efficiencies. The transfection efficiency of supercoiled plasmid DNA is higher compared to nicked circular or linear plasmid DNA when injected into the cytoplasm, however if these forms are directly introduced to the nucleus, this dependency is absent [46]. Therefore DNA stability in the cytoplasm is important to achieving successful transfection and must be considered since cells must uptake the DNA into the cytoplasm before they can enter the nuclear pore complexes. There is potential for developing a better cationic agent than Lipofectamine 2000® that can better protect the plasmid DNA from degradation in the cytoplasm, thereby increasing the transfection efficiency. Endocytosis is hypothesized to be the manner in which DNA complexed to nanoparticles is internalized by the cellular environment [36]. When endocytosis is inhibited, transfection efficiency is reduced [36]. Therefore, the transfection efficiencies demonstrated in this study could be improved if the endocytosis pathway by which the DNA-Lipoplexes enter the cells is ascertained, since there are there are several possible pathways of entry into the cells [45,47]. The development of an improved cationic agent that targets and enhances the type of endocytosis utilized by the cells could also increase transfection efficiency.

There are a number of material factors that can be used to increase transfection efficiency. DNA and calcium phosphate coprecipitation is influenced by concentrations of calcium and phosphate, DNA concentrations, temperature, and reaction time [23]. The mSBF contained Mg, which may have impeded the coprecipitation of the DNA-Lipoplexes resulting in relatively low transfection efficiencies. Changing the composition of the mineralizing solutions by removing Mg could alter the transfection efficiency [20]. Concentrations of calcium and phosphate in solution may also affect the concentration of DNA-Lipoplexes that coprecipitate with the calcium phosphate [23]. Therefore, changing the supersaturation of the mSBF could change the transfection efficiency. Changing the composition of the mineralization solution can also change the rate of DNA release [20], which suggests that apatite dissolution affects DNA release. The differences in transfection efficiency can also be influenced by the surface morphology and DNA retention at the mineral surface. Additionally, the ratio of DNA to lipid and type of lipid can be altered. In cationic lipid mediated transfection, the higher the lipid dosage, the higher the transfection efficiency [43]. In this study, a commercial lipid agent was used as a model for developing a DNA-Lipoplex coprecipitation system. Designing a cationic lipid that can better protect supercoiled DNA, increase cellular internalization, and prevent degradation from occurring upon uptake would further the development of a feasible non-viral gene delivery method.

5. Conclusion

At standard temperatures, pressures and physiological pH, coprecipitation was used to incorporate plasmid DNA complexed with a cationic lipid into a biomimetic apatite. The stability of the plasmid DNA-Lipoplexes is retained during coprecipitation and the complexes are colocalized on the mineralized polymer substrates. DNA-Lipoplex coprecipitation resulted in a higher transfection efficiency in comparison to other methods of delivery, including adsorption of DNA-Lipoplexes. By combining the methods of calcium phosphate based precipitation and cationic lipid assisted transfection, a gene delivery method was developed that has the ability to combine osteoconductivity and osteoinductivity. The coprecipitation of DNA-Lipoplexes into biomimetically nucleated apatite has the potential to be used in bone regeneration and allows for more control over the cellular behavior *in vivo*.

Acknowledgments

This research is supported by NIH DE 015411 (DHK), DE 13380 (DHK), and the Tissue Engineering at Michigan Grant T32 DE007057 (LNL). The authors would like to thank the University of Michigan Electron Microbeam Analysis Laboratory for the use of their scanning electron microscope. The authors would also like to thank Viral Patel for aid in plasmid DNA preparation and purification.

References

1. Hench LL. Bioceramics - from Concept to Clinic. J Am Ceram Soc 1991;74:1487–1510.
2. Murphy WL, Kohn DH, Mooney DJ. Growth of continuous bonelike mineral within porous poly (lactide-co-glycolide) scaffolds in vitro. J Biomed Mater Res 2000;50:50–58. [PubMed: 10644963]
3. Kohn, DH.; Shin, K.; Hong, SI.; Jayasuriya, AC.; Leonova, EV.; Rossello, RA., et al. Self-Assembled Mineral Scaffolds as Model Systems for Biomineralization and Tissue Engineering. In: Landis, WJ.; Sodek, J., editors. Proceedings of the Eighth International Conference on the Chemistry and Biology of Mineralized Tissues. Toronto, Canada: University of Toronto Press; 2005.
4. Murphy WL, Peters MC, Kohn DH, Mooney DJ. Sustained release of vascular endothelial growth factor from mineralized poly(lactide-co-glycolide) scaffolds for tissue engineering. Biomaterials 2000;21:2521–2527. [PubMed: 11071602]
5. Liu Y, Hunziker EB, Randall NX, de Groot K, Layrolle P. Proteins incorporated into biomimetically prepared calcium phosphate coatings modulate their mechanical strength and dissolution rate. Biomaterials 2003;24:65–70. [PubMed: 12417179]

6. Stigter M, de Groot K, Layrolle P. Incorporation of tobramycin into biomimetic hydroxyapatite coating on titanium. Biomaterials 2002;23:4143–4153. [PubMed: 12182316]
7. Liu YL, Layrolle P, de Bruijn J, van Blitterswijk C, de Groot K. Biomimetic coprecipitation of calcium phosphate and bovine serum albumin on titanium alloy. J Biomed Mater Res 2001;57:327–335. [PubMed: 11523027]
8. Wen HB, Wolke JG, de Wijn JR, Liu Q, Cui FZ, de Groot K. Fast precipitation of calcium phosphate layers on titanium induced by simple chemical treatments. Biomaterials 1997;18:1471–1478. [PubMed: 9426176]
9. Wen HB, de Wijn JR, Cui FZ, de Groot K. Preparation of calcium phosphate coatings on titanium implant materials by simple chemistry. J Biomed Mater Res 1998;41:227–236. [PubMed: 9638527]
10. Wen HB, van den Brink J, de Wijn JR, Cui FZ, de Groot K. Crystal growth of calcium phosphate on chemically treated titanium. J Cryst Growth 1998;186:616–623.
11. Wen HB, de Wijn JR, van Blitterswijk CA, de Groot K. Incorporation of bovine serum albumin in calcium phosphate coating on titanium. J Biomed Mater Res 1999;46:245–252. [PubMed: 10380003]
12. Liu YL, Hunziker EB, Layrolle P, De Bruijn JD, De Groot K. Bone morphogenetic protein 2 incorporated into biomimetic coatings retains its biological activity. Tissue Eng 2004;10:101–108. [PubMed: 15009935]
13. Liu Y, de Groot K, Hunziker EB. BMP-2 liberated from biomimetic implant coatings induces and sustains direct ossification in an ectopic rat model. Bone 2005;36:745–757. [PubMed: 15814303]
14. Luong LN, Hong SI, Patel RJ, Outslay ME, Kohn DH. Spatial control of protein within biomimetically nucleated mineral. Biomaterials 2006;27:1175–1186. [PubMed: 16137760]
15. Partridge KA, Oreffo ROC. Gene delivery in bone tissue engineering: Progress and prospects using viral and nonviral strategies. Tissue Eng 2004;10:295–307. [PubMed: 15009954]
16. Huang YC, Simmons C, Kaigler D, Rice KG, Mooney DJ. Bone regeneration in a rat cranial defect with delivery of PEI-condensed plasmid DNA encoding for bone morphogenetic protein-4 (BMP-4). Gene Ther 2005;12:418–426. [PubMed: 15647766]
17. Park J, Ries J, Gelse K, Kloss F, von der Mark K, Wiltfang J, et al. Bone regeneration in critical size defects by cell-mediated BMP-2 gene transfer: a comparison of adenoviral vectors and liposomes. Gene Ther 2003;10:1089–1098. [PubMed: 12808439]
18. Schek RM, Hollister SJ, Krebsbach PH. Delivery and protection of adenoviruses using biocompatible hydrogels for localized gene therapy. Mol Ther 2004;9:130–138. [PubMed: 14741786]
19. Leong KW, Mao HQ, Truong-Le VL, Roy K, Walsh SM, August JT. DNA-polycation nanospheres as non-viral gene delivery vehicles. J Control Release 1998;53:183–193. [PubMed: 9741926]
20. Shen H, Tan J, Saltzman WM. Surface-mediated gene transfer from nanocomposites of controlled texture. Nat Mater 2004;3:569–574. [PubMed: 15258575]
21. Shea LD, Smiley E, Bonadio J, Mooney DJ. DNA delivery from polymer matrices for tissue engineering. Nat Biotechnol 1999;17:551–554. [PubMed: 10385318]
22. Mountain A. Gene therapy: the first decade. Trends Biotechnol 2000;18:119–128. [PubMed: 10675899]
23. Jordan M, Schallhorn A, Wurm FM. Transfecting mammalian cells: Optimization of critical parameters affecting calcium-phosphate precipitate formation. Nucleic Acids Res 1996;24:596–601. [PubMed: 8604299]
24. Kofron MD, Laurencin CT. Development of a calcium phosphate co-precipitate/poly(lactideco-glycolide) DNA delivery system: release kinetics and cellular transfection studies. Biomaterials 2004;25:2637–2643. [PubMed: 14751750]
25. Lv HT, Zhang SB, Wang B, Cui SH, Yan J. Toxicity of cationic lipids and cationic polymers in gene delivery. J Control Release 2006;114:100–109. [PubMed: 16831482]
26. Yi SW, Yune TY, Kim TW, Chung H, Choi YW, Kwon IC, et al. A cationic lipid emulsion/DNA complex as a physically stable and serum-resistant gene delivery system. Pharm Res 2000;17:314–320. [PubMed: 10801220]
27. Gao X, Huang L. A novel cationic liposome reagent for efficient transfection of mammalian cells. Biochem Biophys Res Commun 1991;179:280–285. [PubMed: 1883357]

28. Park J, Lutz R, Felszeghy E, Wiltfang J, Nkenke E, Neukam FW, et al. The effect on bone regeneration of a liposomal vector to deliver BMP-2 gene to bone grafts in peri-implant bone defects. Biomaterials 2007;28:2772–2782. [PubMed: 17339051]
29. Kong HJ, Liu JD, Riddle K, Matsumoto T, Leach K, Mooney DJ. Non-viral gene delivery regulated by stiffness of cell adhesion substrates. Nat Mater 2005;4:460–464. [PubMed: 15895097]
30. Gazit D, Turgeman G, Kelley P, Wang E, Jalenak M, Zilberman Y, et al. Engineered pluripotent mesenchymal cells integrate and differentiate in regenerating bone: A novel cell-mediated gene therapy. J Gene Med 1999;1:121–133. [PubMed: 10738576]
31. Shea CM, Edgar CM, Einhorn TA, Gerstenfeld LC. BMP treatment of C3H10T1/2 mesenchymal stem cells induces both chondrogenesis and osteogenesis. J Cell Biochem 2003;90:1112–1127. [PubMed: 14635186]
32. Blessing T, Remy JS, Behr JP. Monomolecular collapse of plasmid DNA into stable virus-like particles. Proc Natl Acad Sci U S A 1998;95:1427–1431. [PubMed: 9465031]
33. Banerjee R, Das PK, Srilakshmi GV, Chaudhuri A, Rao NM. Novel series of non-glycerol-based cationic transfection lipids for use in liposomal gene delivery. J Med Chem 1999;42:4292–4299. [PubMed: 10543873]
34. Segura T, Shea LD. Surface-tethered DNA complexes for enhanced gene delivery. Bioconjug Chem 2002;13:621–629. [PubMed: 12009954]
35. Dworetzky SI, Lanford RE, Feldherr CM. The effects of variations in the number and sequence of targeting signals on nuclear uptake. J Cell Biol 1988;107:1279–1287. [PubMed: 3170630]
36. Luo D, Saltzman WM. Enhancement of transfection by physical concentration of DNA at the cell surface. Nat Biotechnol 2000;18:893–895. [PubMed: 10932162]
37. Schmidt T, Friehs K, Schleef M, Voss C, Flaschel E. Quantitative analysis of plasmid forms by agarose and capillary gel electrophoresis. Anal Biochem 1999;274:235–240. [PubMed: 10527521]
38. Cherng JY, Schuurmans-Nieuwenbroek NM, Jiskoot W, Talsma H, Zuidam NJ, Hennink WE, et al. Effect of DNA topology on the transfection efficiency of poly((2-dimethylamino)ethyl methacrylate)-plasmid complexes. J Control Release 1999;60:343–353. [PubMed: 10425339]
39. Chancham P, Hughes JA. Relationship between plasmid DNA topological forms and in vitro transfection. J Liposome Res 2001;11:139–152. [PubMed: 19530929]
40. Hansma HG, Golan R, Hsieh W, Lollo CP, Mullen-Ley P, Kwoh D. DNA condensation for gene therapy as monitored by atomic force microscopy. Nucleic Acids Res 1998;26:2481–2487. [PubMed: 9580703]
41. Golan R, Pietrasanta LI, Hsieh W, Hansma HG. DNA toroids: Stages in condensation. Biochemistry (N Y) 1999;38:14069–14076.
42. Okazaki M, Yoshida Y, Yamaguchi S, Kaneno M, Elliott JC. Affinity binding phenomena of DNA onto apatite crystals. Biomaterials 2001;22:2459–2464. [PubMed: 11516076]
43. Kim SW, Ogawa T, Tabata Y, Nishimura I. Efficacy and cytotoxicity of cationic-agent-mediated nonviral gene transfer into osteoblasts. J Biomed Mater Res A 2004;71A:308–315. [PubMed: 15372469]
44. Park MS, Kim SS, Cho SW, Choi CY, Kim BS. Enhancement of the osteogenic efficacy of osteoblast transplantation by the sustained delivery of basic fibroblast growth factor. J Biomed Mater Res B Appl Biomater 2006;79B:353–359. [PubMed: 16924630]
45. Prasad TK, Rangaraj N, Rao NM. Quantitative aspects of endocytic activity in lipid-mediated transfections. FEBS Lett 2005;579:2635–2642. [PubMed: 15862302]
46. Remaut K, Sanders NN, Fayazpour F, Demeester J, De Smedt SC. Influence of plasmid DNA topology on the transfection properties of DOTAP/DOPE lipoplexes. J Control Release 2006;115:335–343. [PubMed: 17010468]
47. Wasungu L, Hoekstra D. Cationic lipids, lipoplexes and intracellular delivery of genes. J Control Release 2006;116:255–264. [PubMed: 16914222]

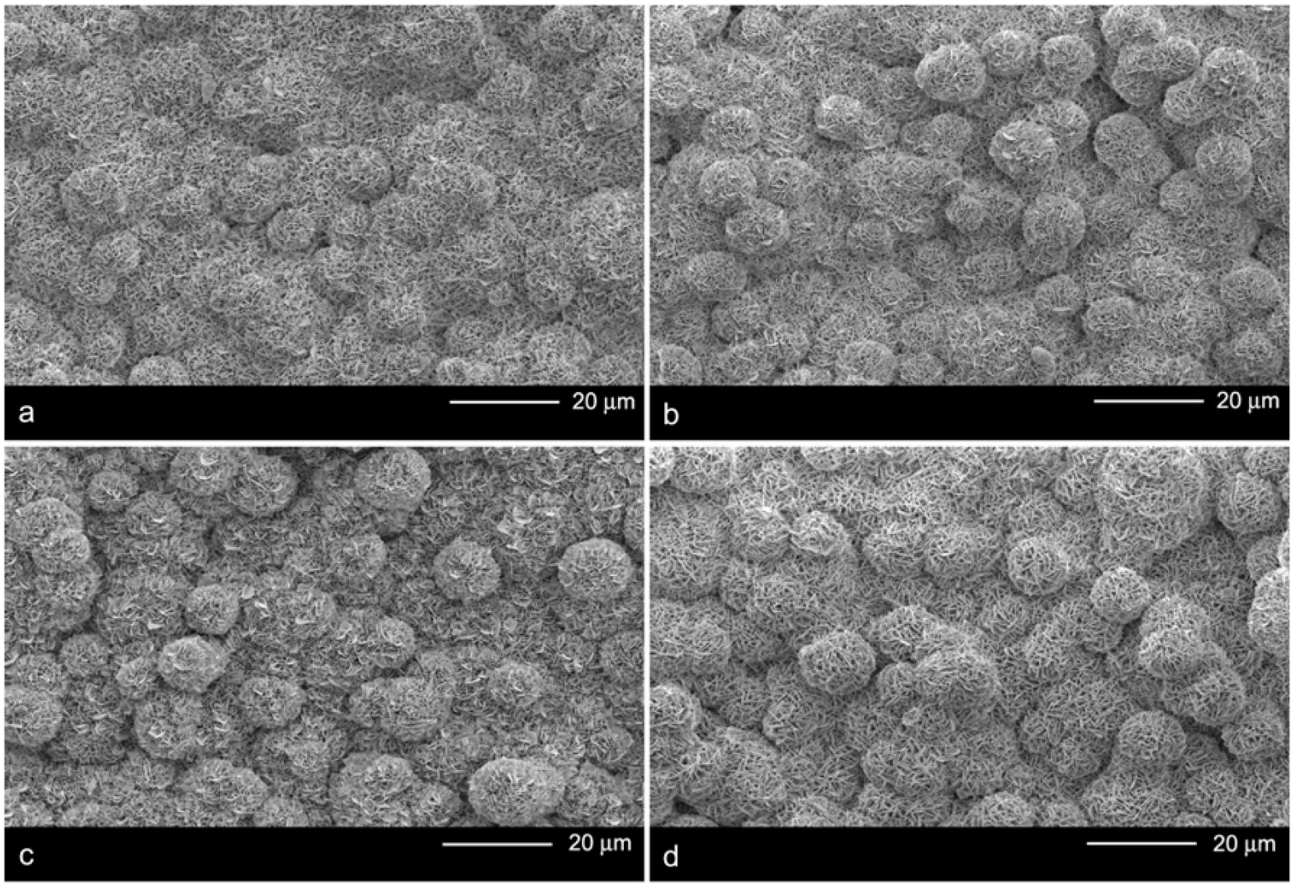

Figure 1.
Low magnification SEM images of the bone-like mineral surface following different DNA incorporation methods: a) Mineralized control b) Plasmid DNA coprecipitation c) DNA-Lipoplex adsorption and d) DNA-Lipoplex coprecipitation. Neither coprecipitation group demonstrated a difference in the size of the mineral nucleation sites as compared to the mineralized controls.

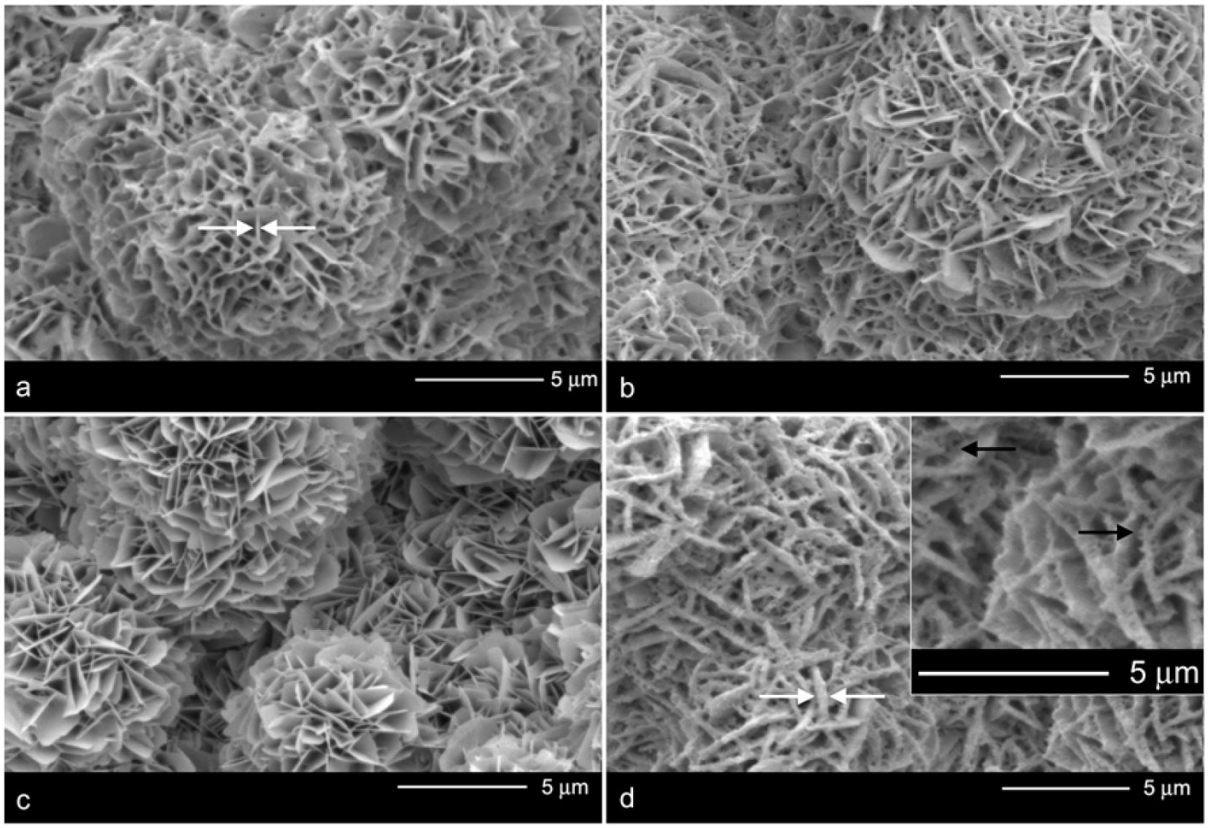

Figure 2.
High magnification SEM images of the bone-like mineral surface following different DNA incorporation methods: a) Mineralized control b) Plasmid DNA coprecipitation c) DNA-Lipoplex adsorption and d) DNA-Lipoplex coprecipitation. DNA-Lipoplex incorporation via coprecipitation leads to the thickening (white arrows) of the plate-like mineral structures. The "fibrous" coating (black arrows in inset) is most likely due to presence of the cationic lipid because the coprecipitation of DNA alone resulted in minimal changes in apatite morphology.

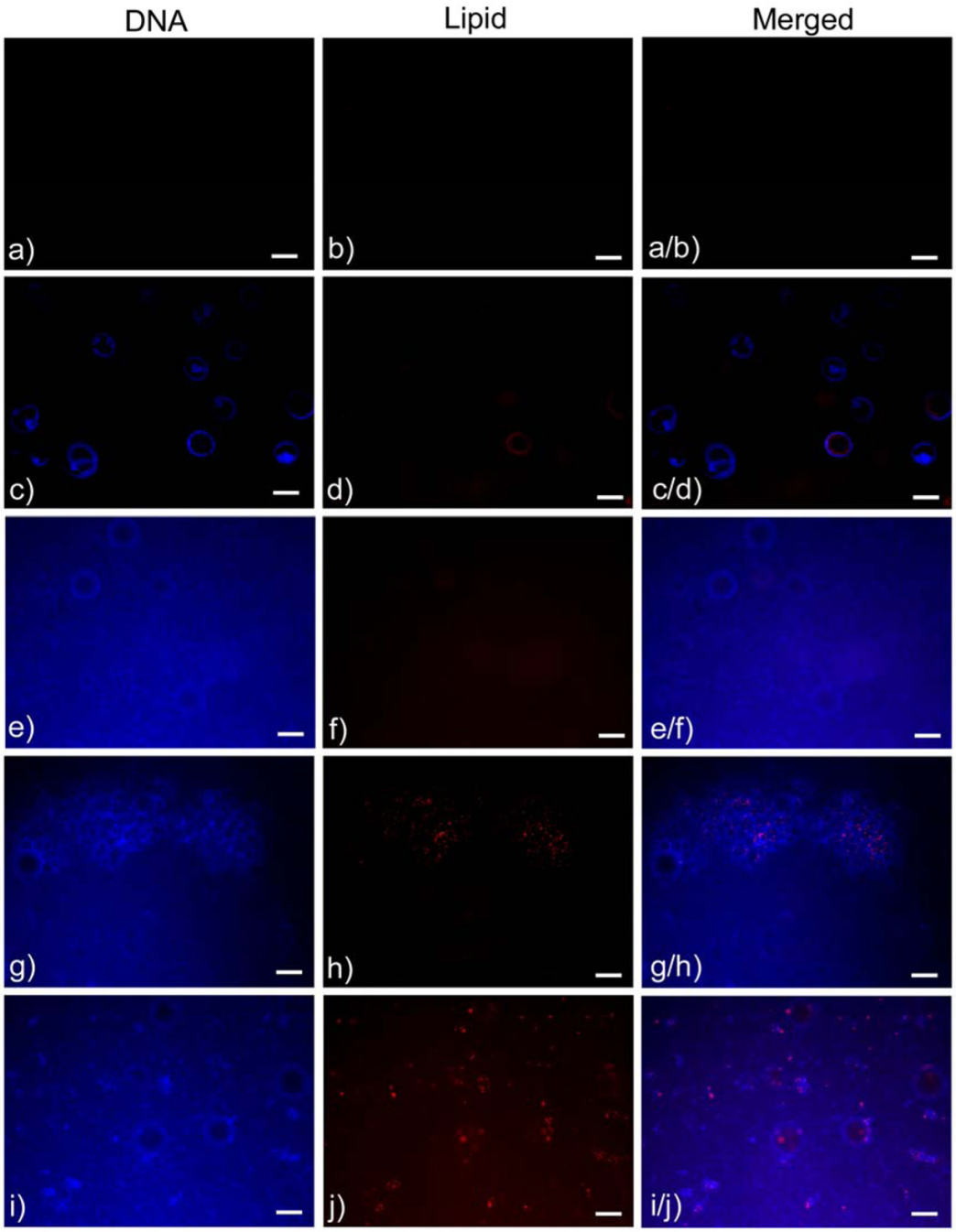

Figure 3.
Fluorescence images of DNA and lipid agent components from representative samples from each of the following groups: a–b) Mineralized controls, c–d) Plasmid DNA incorporated into PLGA, e–f) Plasmid DNA coprecipitated with mineral, g–h) Plasmid DNA-Lipoplex adsorbed to mineralized films, and i–j) Plasmid DNA-Lipoplex coprecipitated with mineral. Distribution of both the plasmid DNA and the lipid transfection agent on the bone-like mineral was demonstrated by the colocalization of the fluorescent staining (after thorough rinsing) in the adsorption and coprecipitation groups and the absence of staining in the mineralized controls. Scale bars represent 100 μm.

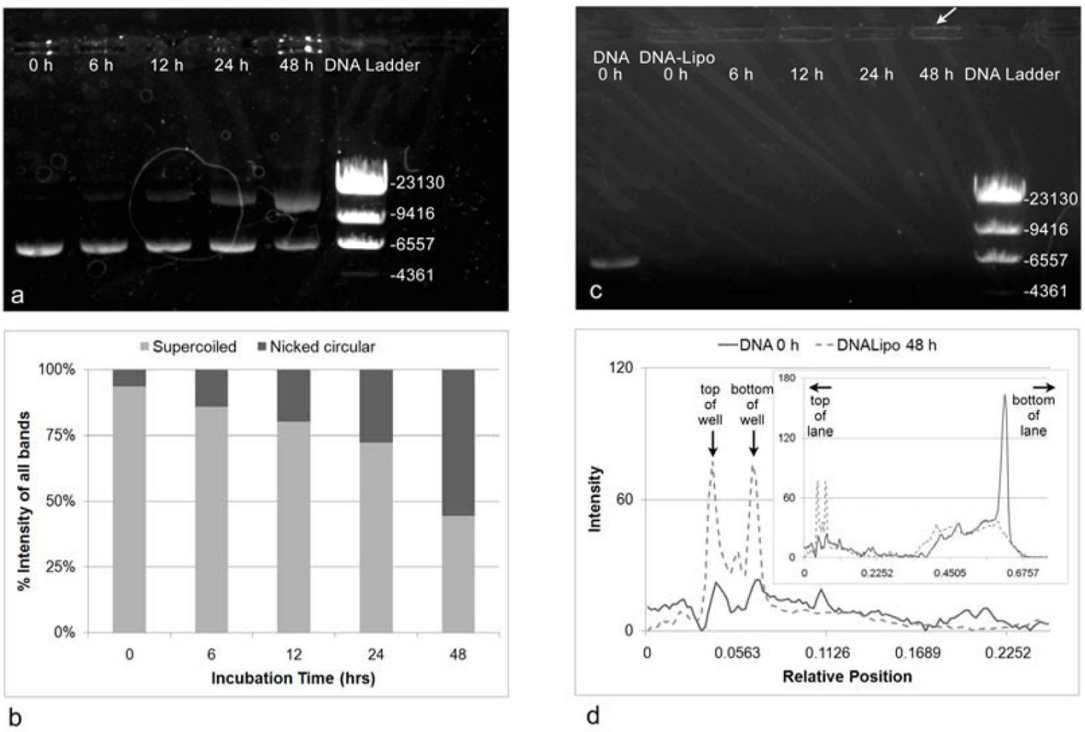

Figure 4.

Plasmid DNA stability in water, as indicated by a) gel electrophoresis and b) quantification of relative percentages of different forms of DNA. The total intensity of all bands of interest (supercoiled and nicked circular DNA) is equivalent to 100% at each incubation time. Stability of DNA decreases with increasing incubation time as demonstrated by the increasing intensity of the top band (between 23130 and 9416, nicked circular form of DNA) and decreasing intensity of the bottom band, ca. 6557 (supercoiled form of the plasmid DNA). c) DNA-Lipoplex stability in Opti-Mem. Complexation of the DNA and lipid was almost complete due to the absence of bands in these groups. Due to size exclusion, the complexes were not able to leave the wells, resulting in the brightness (white arrow) surrounding the wells. d) Intensity profiles for 2 lanes of the gel: DNA 0 h and DNA-Lipo 48 h demonstrate that the peaks that appear for these wells represent the edges of the wells. Peak intensities for the DNA-Lipoplexes are higher compared to DNA only. Profile intensities for the entire lanes are shown in the inset image.

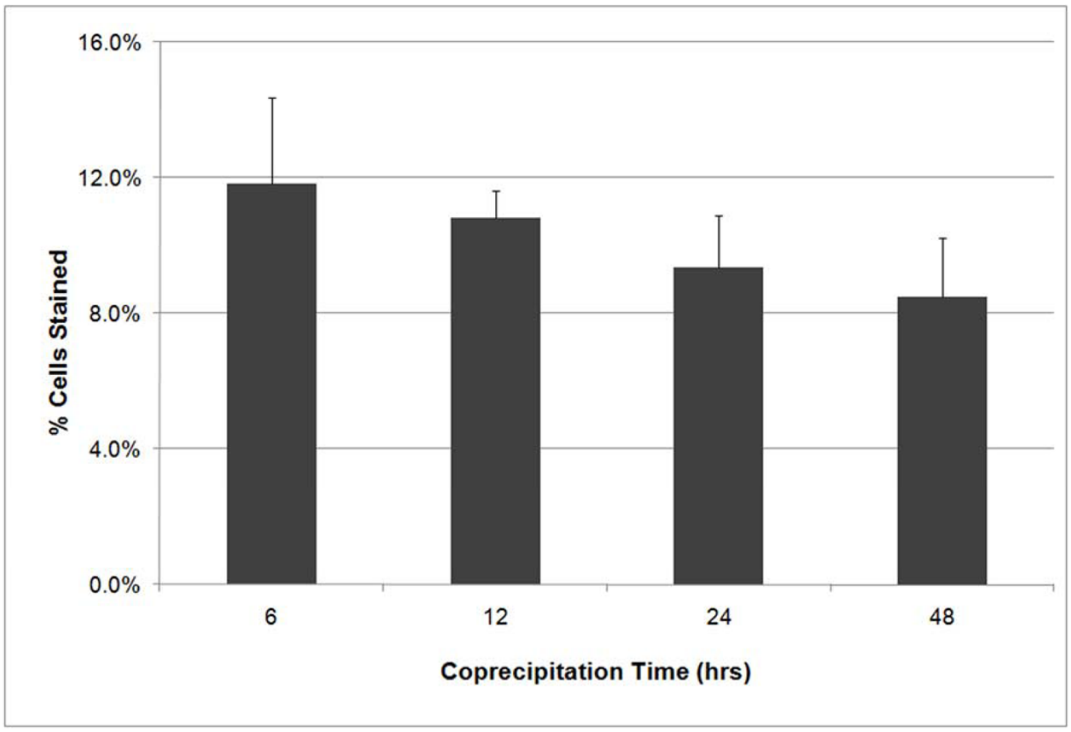

Figure 5.
Transfection efficiency of DNA-Lipoplexes based on the period of coprecipitation: 6 h, 12 h, 24 h, and 48 h. No significant differences in transfection efficiency existed between coprecipitation times (ANOVA, n=4, p=0.084).

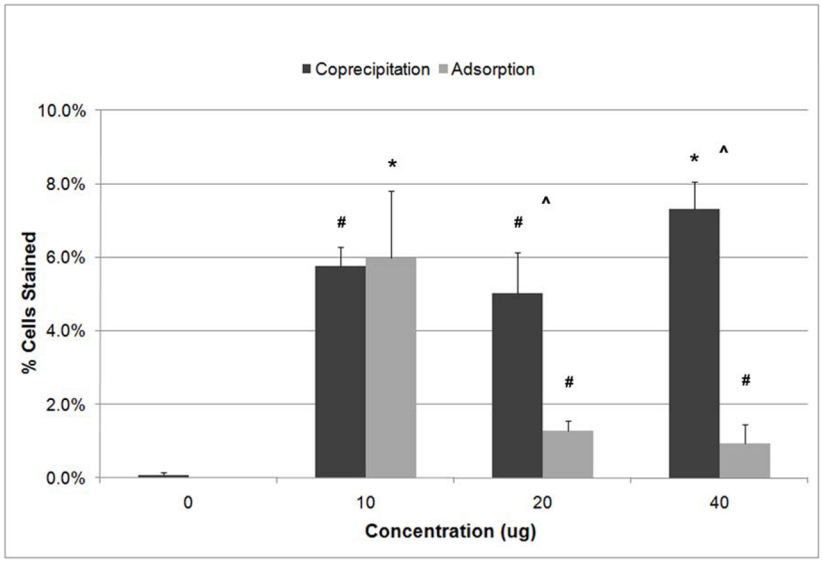

Figure 6.

Significant differences in transfection efficiencies with concentration of DNA-Lipoplexes were demonstrated for adsorption and coprecipitation groups, $p=0.004$ (ANOVA on Ranks, $n=4$) and $p<0.001$ (ANOVA, $n=4$) respectively. Highest transfection efficiency resulted when 10 μg was adsorbed (SNK, $p<0.05$ relative to other adsorption concentrations) and 40 μg/ml was coprecipitated (SNK, $p\leq0.009$ relative to other coprecipitation concentrations). Comparison of adsorption and coprecipitation at the same concentrations demonstrated a higher efficiency for the coprecipitation groups at 20 μg and 40 μg (SNK, $p<0.05$ for both concentrations). The higher retention of complexes on the apatite surface for the coprecipitation group leads to a higher surface density, and therefore results in a higher transfection efficiency. ^ represents $p<0.05$ between coprecipitation and adsorption at a given concentration, # represents $p<0.05$ in comparison to the concentration of 0, and * represents $p<0.05$ in comparison to all other concentrations within the same technique (either adsorption or coprecipitation).

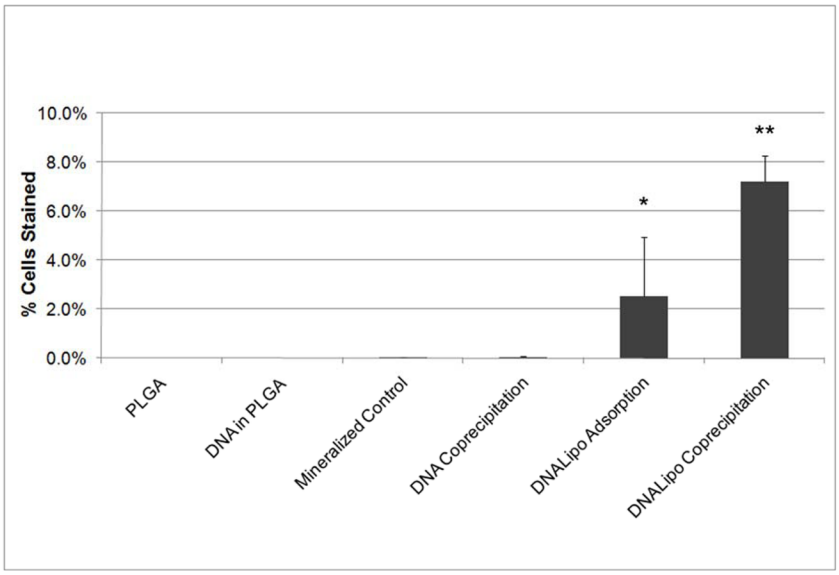

Figure 7.

DNA-Lipoplex coprecipitation resulted in the highest transfection efficiency compared to all other groups (SNK, n=4, $p<0.05$). The higher transfection efficiency of the DNA-Lipoplex adsorption group compared to the DNA only coprecipitation group suggests that the addition of the cationic lipid enhances transfection. Higher transfection efficiency for coprecipitation compared to adsorption suggests higher retention of the complexes on the surface of the apatite. * represents $p<0.05$ in comparison to each of the groups to the left, ** represents $p<0.05$ in comparison to each of the groups to the left.